European Journal of Nuclear Medicine and Molecular Imaging (2019) 46:810–820
https://doi.org/10.1007/s00259-018-4251-5

ORIGINAL ARTICLE

Prospective comparison of (4*S*)-4-(3-^{18}F-fluoropropyl)-L-glutamate versus ^{18}F-fluorodeoxyglucose PET/CT for detecting metastases from pancreatic ductal adenocarcinoma: a proof-of-concept study

Mei-Fang Cheng[1] · Ya-Yao Huang[1] · Bing-Ying Ho[2,3] · Ting-Chun Kuo[2] · Ling-Wei Hsin[4,5,6] · Chyng-Yann Shiue[1,5] · Hsun-Chuan Kuo[2] · Yung-Ming Jeng[7] · Rouh-Fang Yen[1] · Yu-Wen Tien[2]

Received: 12 October 2018 / Accepted: 26 December 2018 / Published online: 11 January 2019

Abstract

Purpose (4*S*)-4-(3-^{18}F-Fluoropropyl)-L-glutamate (FSPG) positron emission tomography (PET) reflects system x_C^- transporter (xCT) expression. FSPG PET has been used to detect brain, lung, breast and liver cancer with only modest success. There is no report on the use of FSPG PET in pancreatic ductal adenocarcinoma (PDAC), presumably because of normal xCT expression in the pancreas. Nonetheless, the tissue-specific expression of xCT in the pancreas suggests that FSPG PET may be ideal for identifying metastasized PDAC.

Methods The performance of FSPG in detecting PDAC metastases was compared with that of ^{18}F-fluorodeoxyglucose (FDG) in small-animal PET studies in seven PDAC tumour-bearing mice and in prospective PET/computed tomography (CT) studies in 23 patients with tissue-confirmed PDAC of stage III or stage IV. All PET/CT results were correlated with the results of histopathology or contrast-enhanced CT (ceCT) performed 3 and 6 months later.

Results In the rodent model, FSPG PET consistently found more PDAC metastases earlier than FDG PET. FSPG PET showed a trend for a higher sensitivity, specificity and diagnostic accuracy than FDG PET in detecting PDAC metastases in a patient-based analysis: 95.0%, 100.0% and 95.7%, and 90.0%, 66.7% and 90.0%, respectively. In a lesion-based analysis, FSPG PET identified significantly more PDAC metastases, especially in the liver, than FDG PET (109 vs. 95; $P = 0.0001$, 95% CI 4.9–14.6). The tumour-to-background ratios for FSPG and FDG uptake on positive scans were similar (FSPG 4.2 ± 4.3, FDG 3.6 ± 3.0; $P = 0.44$, 95% CI −1.11 to 0.48), despite a lower tumour maximum standardized uptake value in FSPG-avid lesions (FSPG 4.2 ± 2.3, FDG 7.7 ± 5.7; $P = 0.002$, 95% CI 0.70–4.10). Because of the lower physiological activity of FSPG in the liver, FSPG PET images of the liver are more easy to interpret than FDG PET images, and therefore the use of FSPG improves the detection of liver metastasis.

Conclusion FSPG PET is superior to FDG PET in detecting metastasized PDAC, especially in the liver.

Keywords Pancreatic cancer · Liver metastases · Positron emission tomography · FSPG · xC transporter system

Electronic supplementary material The online version of this article (https://doi.org/10.1007/s00259-018-4251-5) contains supplementary material, which is available to authorized users.

✉ Yu-Wen Tien
ywtien5106@ntu.edu.tw

[1] Department of Nuclear Medicine, National Taiwan University Hospital and National Taiwan University College of Medicine, Taipei, Taiwan

[2] Department of Surgery, National Taiwan University Hospital and National Taiwan University College of Medicine, 7 Chung-Shan South Rd., Taipei 10002, Taiwan, Republic of China

[3] Department of Anesthesiology, Wang Fang Hospital, Taipei Medical University, Taipei, Taiwan

[4] School of Pharmacy, National Taiwan University, Taipei, Taiwan

[5] Molecular Imaging Center, National Taiwan University, Taipei, Taiwan

[6] Center for Innovative Therapeutics Discovery, National Taiwan University, Taipei, Taiwan

[7] Department of Pathology, National Taiwan University Hospital and National Taiwan University College of Medicine, Taipei, Taiwan

Introduction

Surgery is the only potentially curative treatment for patients with pancreatic ductal adenocarcinoma (PDAC) [1–3]. However, despite the use of adjuvant therapies, most patients who initially undergo curative resection still face a high rate of postoperative recurrence, with a median disease-free survival of only 11–20 months and an estimated 5-year survival rate of 27% in the USA [4–6]. Studies have shown that the initial site of recurrence is the liver in 70% of patients, and more than half of the recurrences develop during the first 6 months postoperatively. The fact that liver metastases develop so soon after surgery suggests that cancer cells may have already metastasized to the liver at the time of diagnosis, but current imaging tools are not sensitive enough to detect these metastases [4]. Although positron emission tomography (PET) with ^{18}F-fluorodeoxyglucose (FDG) is uniquely able to evaluate cellular metabolism, it is not adequate for preoperative staging of PDAC [7]. A study to determine the impact of FDG PET/computed tomography (CT), compared to contrast-enhanced CT (ceCT), on the management of 46 patients with presumed resectable PDAC found only one (1/5, 20.0%) additional liver metastasis [8], which is far less than the reported incidence of liver recurrence after resection. Therefore, a more sensitive radiotracer than FDG is needed to detect liver metastases from PDAC and avoid unnecessary or even harmful pancreatectomy.

The x_C^- system is a heterodimeric transporter (xCT) that mediates sodium-independent cellular uptake of cystine in exchange for intracellular glutamate at the plasma membrane, a process crucial in the detoxification of reactive oxygen species (ROS) in proliferating tumours [9–11]. In a study of normal human cells and tissues, xCT was found to be predominantly expressed in the brain, pancreas, and stromal and immune cells, but not in organs preferentially metastasized from PDAC such as the liver, lung and bone [12]. Although xCT is not expressed in normal liver and lung, it has been reported to be expressed in hepatocellular carcinoma (HCC), breast cancer and lung cancer, especially in those with a CD44 splice variant [13]. xCT plays an important role in the regulation of the redox status in cancer cells.

(4*S*)-4-(3-^{18}F-Fluoropropyl)-L-glutamate (FSPG) is a PET tracer designed to image xCT activity [14, 15]. Based on cancer-specific upregulation of xCT expression, FSPG PET has been used for the detection of brain, breast, lung and liver cancer [14, 16–19]. However, these published trials showed only a modest effect, which may account for the lack of further reports on the clinical use of FSPG PET. In contrast, the high expression of xCT in normal pancreas precludes the use of FSPG PET in PDAC. On the other hand, if tissue-specific expression of xCT in normal pancreas is not lost, but is upregulated during malignant transformation and metastasis, FSPG PET would be an ideal tool to detect metastasized PDAC (based on both cancer-upregulated and tissue-specific expression of xCT).

PDAC is notorious for its poor prognosis because of early metastasis and tumour extension along vessels and nerves. We searched MEDLINE and ClinicalTrials.gov (ClinicalTrials.gov) and found no trials investigating the use of FSPG PET in PDAC. For clinicians, accurate staging, especially identification of occult metastasis, is even more important than the detection of a small primary tumour. Based on tissue-specific expression of xCT in normal pancreas, we conducted preclinical and clinical trials to test whether FSPG PET can detect PDAC metastases undetectable by ceCT or even FDG PET.

Materials and methods

To determine if xCT expression in normal pancreatic tissue is lost during malignant transformation or metastases, we measured xCT expression by anti-xCT immunohistochemical (IHC) staining in paired samples of normal pancreas and PDAC (from six patients), and in paired samples of normal liver and PDAC liver metastases (from two patients). We further performed immunofluorescent (IF) staining for xCT in normal human pancreatic ductal epithelial cells (HPDE/E6E7) and in three pancreatic cancer cell lines (AsPC-1, CFPAC-1 and PANC-1).

Cell culture experiments

Cells and culture

Human pancreatic cancer cell lines (AsPC-1, CFPAC-1, PANC-1, BxPC3, HPAC, HPAF II and SU86·86), normal human pancreatic ductal epithelial cells (HPDE/E6E7), and normal human hepatocytes (WRL-68) were obtained from the American Type Culture Collection (ATCC; Manassas, VA, USA), and cultured in complete growth medium as suggested by the ATCC in an incubator at 37 °C in a humidified atmosphere containing 5% CO_2.

Immunohistochemistry

Sections of formalin-fixed paraffin-embedded paired pancreatic normal and cancer tissues from six patients, and paired normal liver and pancreatic cancer hepatic metastasis from two patients were used for IHC analysis. Heat-induced antigen retrieval was performed using 0.1 M citrate buffer, pH 6.0, with autoclaving for 20 min. Endogenous peroxidase was eliminated using 3% H_2O_2. Slides were blocked with a anti-xCT antibody prepared in-house (A68; 1:100) in phosphate-buffered saline (PBS)/10% fetal bovine serum (FBS) overnight at 4 °C. After washing, the slides were incubated with

horseradish peroxidase rabbit/mouse polymer before visualization with liquid diaminobenzidine tetrahydrochloride plus substrate 3,3′-diaminobenzidine chromogen (Dako REAL EnVision; DAKO GmbH, Jena, Germany). All slides were counterstained with haematoxylin. The images were captured using an Aperio digital pathology system (Leica Biosystems Nussloch GmbH, Nussloch, Germany). Four fields (×400) with xCT negative or high expression were evaluated in each case.

Immunofluorescent staining

Three PDAC cell lines (AsPC-1, PANC-1 and CFPAC-1) and one normal human pancreatic ductal epithelial cell line (HPDE/E6E7) were seeded at 1×10^4 cells per well in 24-well plates. After culture, the cells were washed with PBS and fixed in cold 4% paraformaldehyde solution for 30 min. Nonspecific protein epitopes were blocked using 10% FBS for 1 h. Fixed cells were permeabilized with 0.1% Triton-X-100 in PBS for 30 min. The primary antibody, anti-xCT (1:250; Novus International, St. Louis, MO, USA), was diluted in PBS and incubated with the cells overnight at 4 °C. The secondary antibody, anti-IgG-conjugated Alexa488 (1:500; Thermo Fisher Scientific, Waltham, MA, USA), and 4′,6-diamidino-2-phenylindole (1:50,000; Thermo Fisher Scientific) were diluted with PBS containing Tween and incubated with the cells for 2 h at room temperature. All samples were measured using an Axiovert 200 M inverted microscope (Carl Zeiss, AG, Jena, Germany).

Radiopharmaceuticals

All the FDG and FSPG used in this study was prepared in the PET Radiochemistry Laboratory of National Taiwan University Hospital, which operates in compliance with Current Good Manufacturing Practice regulations and is regularly inspected by the Taiwan Food and Drug Administration. FDG was synthesized as described previously [20]. FSPG was automatically synthesized in a modified GE TRACERlab Fx_{FDG} synthesizer as described previously (GE Healthcare, Wauwatosa, WI, USA; Supplementary Fig. S1) [15, 21].

In vivo study in tumour-bearing mice

Animals

Severe combined immunodeficiency NOD·CB17-Prkdc^{scid}/NcrCrlBltw (NOD-SCID) mice (male, 4–6 weeks old, 18 ± 2 g) were obtained from BioLASCO Taiwan (Taiwan, ROC). All mice were kept in an air-conditioned facility with an artificial 12-h light, 12-h dark cycle (lights on at 6.00 a.m.), and were provided with a standard laboratory diet and filtered water. The mice were acclimated to this environment for at least 1 week prior to study.

An animal model of PDAC liver metastasis was set up by orthotopic injection of 2×10^6 PDAC cells (HPAF II) stably expressing the bioluminescent firefly luciferase (Applied Biological Materials Inc., LV052, Richmond, BC, Canada) into the pancreas of seven NOD-SCID mice. PET imaging was performed 4 weeks after injection of the tumour cells. FSPG and FDG PET/CT imaging studies were performed less than 1 day apart weekly for at least 2 weeks. In vivo bioluminescence imaging (IVIS) using a 200 Series Xenogen IVIS imaging system (Caliper Life Sciences, Alameda, CA, USA) was performed on the second day after completing the last dual tracer imaging. The mice were then killed and tissues were analysed histopathologically.

Small-animal PET imaging and analysis

Prior to PET imaging, all animals were fasted overnight with water provided ad libitum. Small-animal PET imaging (SEDECAL, SA, Madrid, Spain) was performed in animals under 2% isoflurane anaesthesia using a nose cone. A 60-min dynamic imaging scan was started after intravenous injection of 11.1 MBq of FDG or FSPG via a tail vein and was followed by a 10-min CT scan. The list-mode PET data were reconstructed using two-dimensional ordered-subsets expectation maximization reconstruction with CT-based attenuation correction. Images were analysed using PMOD 3.606 software (PMOD Technologies Ltd., Zürich, Switzerland) in a blinded manner. A 40% isocontour volume of interest (VOI) was placed on the area of maximum activity in the tumour lesion, and the maximum standardized uptake value (SUVmax) was computed according to the following formula: (decay-corrected activity/tissue volume) divided by (injected radiotracer activity/body mass), with activity expressed in kilobecquerels, volume in millilitres and mass in grams. Another spherical VOI was placed on the mediastinal blood pool to enable computation of standardized uptake value ratios (SUVRs) of the tumours as tumour/mediastinal blood pool SUVs. Metastases were defined only after confirmation of their appearances at corresponding locations on serial PET scans (4 and 6 weeks after tumour implantation) in addition to histopathological proof.

Studies in patients

Patient selection

This was a prospective open-label, nonrandomized, single-centre, investigator-driven exploratory study to evaluate the performance of FSPG PET/CT in detecting metastases in patients with PDAC. The primary endpoint was to compare the accuracies, as determined in a patient-based analysis and a

lesion-based analysis, of FSPG and FDG PET/CT in detecting metastatic lesions in patients with tissue-proven PDAC. The secondary endpoints were to determine and compare the semiquantification variables from FSPG PET and FDG PET, and to evaluate the safety profile of FSPG and the incidence of adverse reactions to FSPG.

From September 2016 to February 2018, patients diagnosed with stage III (locally advanced) or stage IV (metastatic) PDAC by ceCT at the Department of Surgery of the National Taiwan University Hospital were prospectively enrolled. All patients had histological confirmation of PDAC by endoscopic ultrasound-guided biopsy. Patients aged 20 years or older with Eastern Cooperative Oncology Group performance status ≤2 were invited to participate. Patient inclusion depended on the availability of the FSPG radiotracer in relation to clinical workflow and treatment plans. Patients with another malignancy diagnosed within 5 years, who received abdominal surgery within 3 months, who were pregnant or lactating, or who had an uncontrolled medical disease other than cancer were excluded from the study. Before PET/CT, all patients underwent conventional staging work-up studies, including physical examination, laboratory tests, and abdominal ceCT.

Paired PET/CT imaging

FSPG PET was performed in each patient within a week of FDG PET on the same PET/CT scanner (Discovery PET/CT 710; GE Medical Systems, Milwaukee, WI, USA). FSPG PET was performed before FDG PET in half of the patients (odd numbers) and vice versa (even numbers). No treatment was performed between the two studies. No food restriction is required before FSPG PET [14]. After intravenous injection of 300 MBq of FSPG, FSPG PET images were obtained 60 min after injection (5 min per bed position) from the skull base to the thighs. Patients were encouraged to void their urinary bladder before and after the scan. No intravenous contrast medium was given. The CT component of the PET/CT scanner was used only for attenuation correction and anatomical localization of the PET images. The FDG PET/CT Images were acquired and processed in a manner analogous to that used in a previous study [20].

PET/CT data analysis

FSPG and FDG PET/CT images were reviewed independently in random order, different for the two tracers, during two different sessions, by two nuclear medicine physicians (M.-F.C and R.-F.Y) using the built-in software of the PET/CT system (Xeleris; GE Medical Systems, Milwaukee, WI, USA). The nuclear medicine specialists had >15 years of clinical experience each and were unaware of the results of other diagnostic tests or histology. Diverging interpretations were recorded by a clinical manager, and then resolved by consensus in a consensus reading.

PET/CT images were analysed visually and semiquantitatively in a patient-based and a lesion-based analysis. Abnormal increased tracer activity greater than that of the surrounding background activity not associated with normal structures or artefacts on the PET transaxial slices was analysed visually. The degree of suspicion of an abnormality was recorded using a three-point visual scale: *2* major uptake, *1* minor uptake, and *0* absent uptake [14]. A lesion was classified as positive if it was scored as 1 or 2. The number and location of the areas of abnormal uptake were also recorded in each patient. Six distant metastatic sites were defined prospectively: lungs, liver, peritoneum, skeleton, extra-abdominal lymph nodes, and other organs. Each of these areas counted as one site of metastasis. To avoid excess statistical weighting of patients with diffuse disease, a maximum of five lesions per metastatic site were selected as reference lesions in the lesion-based analysis.

Semiquantitative analysis was performed for each lesion suspected during visual analysis on both FSPG and FDG PET. A spherical VOI of 1.5 cm placed on the area of maximum activity in the tumour lesion was used to determine the SUVmax. Blood pool VOIs were placed on the aorta to define the mean SUV (SUVmean) of the blood pool. The SUVR of each lesion was then derived by calculating the ratio of tumour SUVmax to the SUVmean of the blood pool. When multiple lesions were seen in an organ, the SUVmax and SUVR of the lesion with the highest tracer accumulation were recorded.

Standard of reference

All primary PDAC were histologically confirmed before a patient was enrolled in the present study. Follow-up data were collected for every patient enrolled, including physical examination, histology, medical imaging and biological assays during each clinical visit for at least 3 months. Since biopsy and histopathological confirmation of all metastatic lesions was neither ethical nor practical, a lesion seen on FSPG PET or FDG PET that satisfied one of the following criteria was defined as a true metastasis: histopathological confirmation of metastasis by biopsy; or new or enlarged tumour seen at corresponding locations on ceCT performed 3 or 6 months later. A lesion seen on FSPG PET or FDG PET that did not appear at the corresponding location on ceCT performed 3 or 6 months later was defined as false-positive. Lesions not detected on PET but seen on ceCT and showing progression on follow-up ceCT, or those proven by histopathology, were deemed false-negative. When no follow-up data were available to assess the nature of a lesion, the site of metastasis was excluded from analysis. Radiologists who did not participate in patient recruitment read these ceCT images as part of

routine clinical follow up, unaware of prior PET results. All patients were followed up for at least 6 months or until death.

Safety monitoring

Biochemistry profiles, vital signs and electrocardiograms in all patients were checked before FSPG PET/CT. Vital signs were measured again after completion of the imaging study. All examinations were checked again during each patient's first visit to the outpatient clinic 1 or 2 weeks after imaging. All adverse events were recorded and reported to the National Taiwan University Hospital Ethics Committee.

Statistical analysis

Numerical data are reported as means ± standard deviation, percentages or ranges, unless otherwise specified. The sensitivity, specificity and diagnostic accuracy of FSPG PET and FDG PET in detecting distant metastases according to the patient-based analysis were compared. Quantitative and categorical variables were compared using Student's *t* test and McNemar's test, respectively, and 95% confidence intervals (CI) were determined. A two-tailed *P* value of <0.05 was considered to be statistically significant. Statistical tests were conducted using the JMP® version 5 statistical software package (SAS Institute Inc., Cary, NC, USA).

Study approval

All rodent experiments were performed in compliance with experimental animal care guidelines and the ARRIVE guidelines, and were performed under protocols approved by the Institutional Animal Care and Use Committee and approved by the Laboratory Animal Center of National Taiwan University College of Medicine (no. 20140277).

The clinical study protocol was approved by the National Taiwan University Hospital Ethics Committee (no. 201512084MINC) and the Taiwan Food and Drug Administration, and registered with ClinicalTrials.gov (NCT03144622; ClinicalTrials.gov). All participants underwent PET/CT after providing written informed consent.

Results

Expression of xCT in normal pancreas is not lost during malignant transformation or metastasis

On IHC staining, xCT expression was found to be moderate in normal pancreatic tissue, strong in primary PDAC, weak in normal liver tissue, but strong in PDAC liver metastases (Fig. 1a). IF staining for xCT was seen in all normal and malignant cells (Fig. 1b). These findings indicate that xCT expression in normal pancreas is not lost during malignant transformation or metastasis. Therefore, the use of xCT expression on FSPG PET to trace the migration of PDAC cells is feasible.

Animal studies show FSPG PET, compared to FDG PET, detects more PDAC liver metastases both earlier and at a higher standardized uptake value ratio

Four weeks after orthotopic injection of PDAC cells FDG PET detected liver metastatic lesions in two (28.5%) of seven mice (Supplementary Table S1). FSPG PET detected not only all liver lesions detected by FDG PET in these two mice, but also additional liver metastatic lesions in another three mice (Supplementary Fig. S2). Six weeks after injection of pancreatic cancer cells, FDG detected two liver metastases in two mice, one liver metastasis in four mice, and no liver metastases in another mouse. All these liver metastases detected by FDG PET were also detected by FSPG PET. FSPG PET also detected liver metastases in an additional mouse. FSPG provided significantly better contrast between tumour and background activity than FDG (FSPG SUVR 4.8 ± 1.4, FDG SUVR 3.0 ± 1.0; $P = 0.02$), even though the SUVmax of FSPG was lower (FSPG SUVmax 1.8 ± 0.9, FDG SUVmax 2.6 ± 0.6; $P = 0.04$; Supplementary Fig. S3). All metastatic lesions seen on PET and IVIS imaging were histopathologically confirmed.

Studies in patients

Patients and safety profile of FSPG PET

A clinical study was performed in 23 PDAC patients. All had tissue-proven PDAC by endoscopic ultrasound-guided biopsy. ceCT performed at the time of diagnosis showed liver metastases (stage IV) in 13 patients and no metastases, but locally advanced PDAC (defined as abutting the superior mesenteric or celiac artery or encasing the artery by more than 180 degrees) in ten patients. The demographic characteristics of these patients are shown in Table 1. All patients tolerated FSPG PET well with no adverse effects observed. Of the 23 patients, 19 (82.6%) had a follow-up ceCT scan performed 3 and 6 months after dual FDG and FSPG PET/CT scans. The remaining four patients (17.4%) had only one follow-up ceCT scan performed 3 months after the dual PET scans because of disease progression.

Patient-based analysis

In this proof-of-concept study, both FSPG and FDG PET successfully identified stage IV disease in all of 13 patients with stage IV PDAC. Of 10 patients with stage III PDAC, 7 (70.0%) were found to have metastatic lesions on follow-up

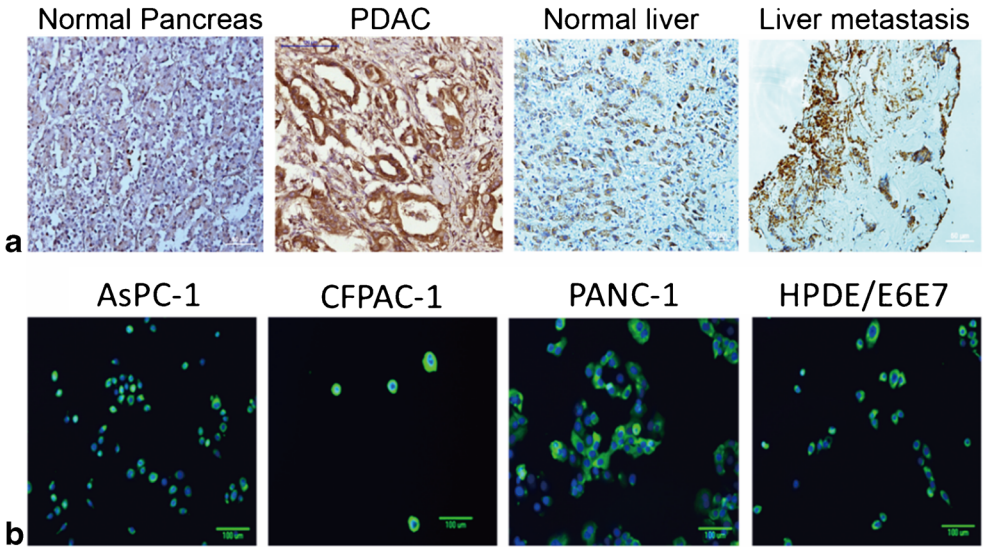

Fig. 1 System x_C^- transporter (xCT) expression in pancreatic tissues and cell lines. **a** Immunohistochemical analysis of normal pancreatic, pancreatic ductal adenocarcinoma (PDAC), normal liver, and PDAC liver metastatic tissues. 3,3′-Diaminobenzidine (DAB) staining (*brown*) shows the strength of xCT expression. Under the same staining conditions, xCT expression in PDAC tissue is stronger than in normal pancreatic tissue. xCT expression in PDAC liver metastatic tissue is also stronger than in normal liver tissue. **b** Immunofluorescent staining of three PDAC cell lines (AsPC-1, CFPAC-1 and PANC-1) and one normal human pancreatic ductal epithelial cell line (HPDE/E6E7) double-stained with xCT (*green*) and 4′,6-diamidino-2-phenylindole (DAPI, *blue*). xCT expression is present in all normal and malignant pancreatic cell lines

Table 1 Demographic characteristics of the 23 patients with pancreatic cancer

Characteristic	Value
Age (years), mean ± SD	62.9 ± 13.3
Sex (M/F), *n*	15/8
Diabetes mellitus, *n* (%)	8 (34.8)
Chronic hepatitis, *n* (%)	5 (21.7)
AST (U/L), median (range)	33 (14–205)
ALT (U/L), median (range)	26 (6–467)
Bilirubin (mg/dL), median (range)	
Total	0.8 (0.4–16.0)
Direct	0.2 (0.1–8.8)
Amylase (U/L), median (range)	43 (20–121)
Lipase (U/L), median (range)	44 (12–341)
Glucose (mg/dL), median (range)	108 (91–183)
CEA (ng/mL), median (range)	6.8 (0.7–251.4)
CA19-9 (U/mL), median (range)	752.6 (2.5–28,921.1)
Tumour location, *n* (%)	
Head	14 (60.9)
Body	8 (34.8)
Tail	1 (4.3)
Stage, *n* (%)	
III	10 (43.5)
IV	13 (56.5)

AST aspartate aminotransferase, *ALT* alanine aminotransferase, *CEA* serum carcinoembryonic antigen, *CA19-9* carbohydrate antigen 19-9

ceCT performed 3 or 6 months after diagnosis. FDG PET correctly identified metastases in 5 of 7 patients (71.4%). One patient had a hepatic abscess misdiagnosed as metastasis by FDG PET (Supplementary Fig. S4). In contrast, FSPG PET detected metastases in 6 of 7 patients (85.7%). The sensitivity, specificity, and diagnostic accuracy of FSPG PET and FDG PET were 95.0%, 100.0% and 95.7%, and 90.0%, 66.7% and 90.0%, respectively. FSPG PET showed higher sensitivity and specificity than FDG PET in detecting PDAC metastases, but the difference was not statistically significant.

Lesion-based analysis

Variable expression of FSPG PET in primary PDAC Primary PDAC were all FDG-avid, but showed variable uptake of FSPG. Physiological FSPG activity in normal pancreatic parenchyma led to an expected decreased visualization of primary PDAC on FSPG PET, as seen in 9 of 23 patients (39.1%). Surprisingly, increased FSPG avidity of the primary PDAC was observed in 14 of 23 patients (60.9%), with a mean SUV of 6.6 ± 1.0 and SUVR of 6.8 ± 2.6 (Fig. 2).

FSPG PET detects more metastases in patients with PDAC than ceCT or FDG PET To avoid statistical bias due to counting, a maximum of five lesions per metastatic site per patient were selected as reference lesions for the lesion-based analysis. All these metastatic lesions were confirmed as metastases by histopathology or their appearance in the corresponding locations

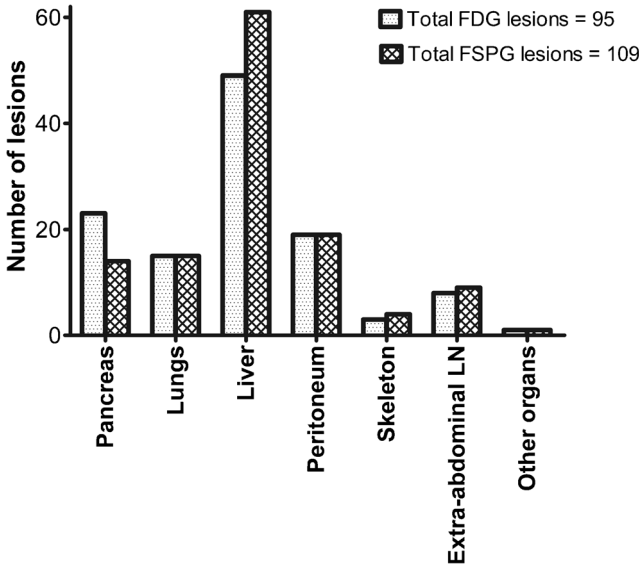

Fig. 2 Total numbers of lesions positive for (4*S*)-4-(3-^{18}F-fluoropropyl)-L-glutamate (^{18}F-FSPG) and ^{18}F-fluorodeoxyglucose (^{18}F-FDG) in various anatomical sites, including the pancreas, lungs, liver, peritoneum, skeleton, extra-abdominal lymph nodes (LN), and other organs

on ceCT performed 3 or 6 months later. At the time of diagnosis, 65 metastatic lesions were detected on initial ceCT in 13 patients with stage IV PDAC (Supplementary Table S2). Follow-up ceCT performed 3 months later detected an additional 39 metastases in patients with stage III PDAC and 40 lesions in patients with stage IV PDAC (Table 2). Together, a total of 144 metastases were found on follow-up ceCT, 78 in the liver (22 in patients with stage III PDAC, 56 in patients with stage IV PDAC).

We evaluated the sensitivity of FSPG and FDG PET in detecting 144 metastatic reference lesions in 23 patients with PDAC (Table 2). The locations of the distant metastases are shown in Fig. 2. The overall sensitivities of FDG and FSPG PET in 144 reference lesions seen on follow-up ceCT in 23 PDAC patients were 66.0% (95/144) and 75.7% (109/144), respectively. In patients initially diagnosed with stage III PDAC, FDG and FSPG PET were able to predict 9 (23.1%) and 17 (43.6%) of 39 metastases, respectively, seen on follow-up ceCT. FSPG PET correctly identified significantly more metastases than FDG PET in patients with stage III PDAC, stage IV PDAC and combined stage III and IV PDAC (Table 2). In patients who showed positive PET lesions, albeit lower metastatic tumour SUVmax on FSPG PET than on FDG PET (FSPG SUVmax 4.2 ± 2.3, FDG SUVmax 7.7 ± 5.7; $P = 0.002$, 95% CI 0.70 to 4.10; Fig. 3a), the lower background FSPG activity rendered the tumour SUVR similar to that of FDG (FSPG SUVR 4.2 ± 4.3, FDG SUVR 3.6 ± 3.0; $P = 0.44$, 95% CI −1.11 to 0.48; Fig. 3b).

Of the 23 patients, 14 (60.7%) had nonhepatic PDAC metastases: 46 lesions were detected on FDG PET and 48 on FSPG PET. In two patients with stage IV PDAC, FSPG PET detected an additional extra-abdominal lymph node metastasis in one and a rib metastasis in the other. Since the difference in detecting nonhepatic PDAC metastases between FSPG and FDG PET was small and the liver is the preferred metastatic organ in PDAC, only those patients with hepatic metastases were analysed.

A total of 78 hepatic metastases were seen on follow-up ceCT: 22 in patients with stage III PDAC and 56 in patients with stage IV PDAC (Table 2). The overall sensitivities of FDG and FSPG PET in identifying 78 reference liver metastases seen on follow-up ceCT in 23 PDAC patients were 62.8% (49/78) and 78.2% (61/78), respectively (Fig. 4). In patients initially diagnosed with locally advanced PDAC (stage III), FDG and FSPG PET predicted 4 (18.2%) and 12 (54.5%) of 22 liver metastases, respectively, seen on follow-up ceCT (Table 2 and Fig. 5). Likewise, FSPG PET correctly identified significantly more hepatic metastases than FDG PET in patients with stage III or combined stage III and IV

Table 2 Number of distant metastases detected in 23 patients with pancreatic cancer

	Positive FDG PET lesions, *n* (%)	Positive FSPG PET lesions, *n* (%)	Follow-up ceCT, *n*	*P* value[a] (95% CI)
All metastases				
Stage III	9 (23.1)	17 (43.6)	39	0.008 (7.8 to 33.2)
Stage IV	86 (81.9)	92 (87.6)	105	0.03 (1.3 to 10.2)
Combined	95 (66.0)	109 (75.7)	144	0.0001 (4.9 to 14.6)
Liver metastases				
Stage III	4 (18.2)	12 (54.5)	22	0.008 (16.3 to 56.5)
Stage IV	45 (80.4)	49 (87.5)	56	NS (0.40 to 13.89)
Combined	49 (62.8)	61 (78.2)	78	0.001 (7.4 to 23.4)

A maximum of five lesions per location were counted per patient to avoid statistical bias

FDG ^{18}F-fluorodeoxyglucose, *PET* positron emission tomography, *FSPG* (4*S*)-4-(3-^{18}F-fluoropropyl)-L-glutamate, *ceCT* contrast-enhanced computed tomography, *CI* confidence interval, *NS* not significant

[a] Comparing true-positives between FSPG and FDG PET/CT using the McNemar χ^2 test

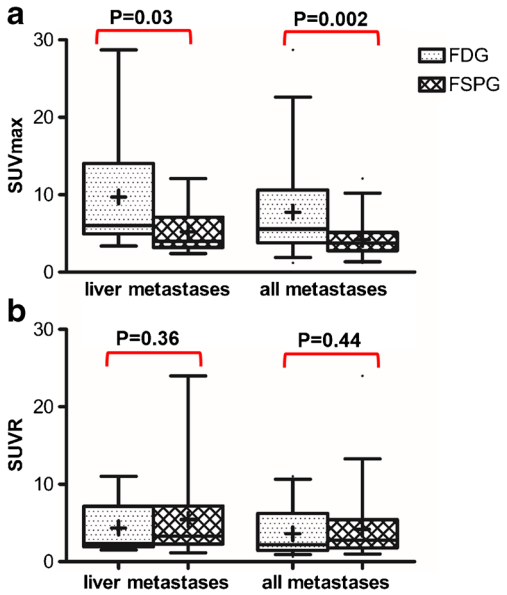

Fig. 3 Tumour maximum standardized uptake values (SUVmax) and tumour-to-blood pool SUV ratios (SUVR) of PET-positive lesions

PDAC (Table 2). Similarly, the hepatic tumour SUVmax of FSPG was lower than that of FDG (FSPG SUVmax 5.2 ± 2.8, FDG SUVmax 9.7 ± 7.4; $P = 0.03$, 95% CI 0.20 to 7.20; Fig. 3a), but the hepatic tumour SUVRs of the two tracers were not significantly different (FSPG SUVR 5.4 ± 5.7, FDG SUVR 4.4 ± 3.4; $P = 0.36$; 95% CI −1.96 to 1.34; Fig. 3b). The lower physiological activity of FSPG in the liver rendered the detection and image interpretation of liver metastasis easier than with FDG PET.

Discussion

As reported elsewhere, we found that FSPG PET was well-tolerated with no adverse events in any of the 23 studied patients [14, 19, 22]. As shown in the patient-based analysis in this study, FSPG PET showed a trend for higher sensitivity, specificity and diagnostic accuracy than FDG PET: 95.0%, 100.0% and 95.7% for FSPG PET, 90.0%, 66.7% and 90.0% for FDG PET, respectively. However, this difference between FSPG PET and FDG PET was not statistically significant owing to the limited number of patients enrolled in this proof-of-concept study. As shown in the lesion-based analysis, FSPG PET identified significantly more PDAC metastases, especially liver metastases, than FDG PET. Detection of metastases not detectable on CT is especially important in patients initially suspected to have only stage III PDAC, as this information will change disease staging and hence the clinical management: FSPG PET detected 17 of 39 metastases (43.6%) not seen on baseline ceCT at least 3 months earlier, whereas FDG PET detected only 9 lesions (23.1%).

The premise of detection of metastasized PDAC by FSPG PET is that expression of xCT in pancreatic tissue is not lost during malignant transformation or metastasis. In accordance with previous reports, we confirmed that xCT expression in normal pancreas (tissue-specific) is not only not lost but also upregulated during malignant transformation and metastasis (cancer-upregulated) [23]. In a clinical trial in ten patients with non-small-cell lung cancer (NSCLC) and five patients with breast cancer, FSPG PET detected 59 (88%) of 67 FDG PET-detected NSCLC lesions and 30 (41%) of 73 FDG PET-detected breast cancer lesions [14]. In another trial in

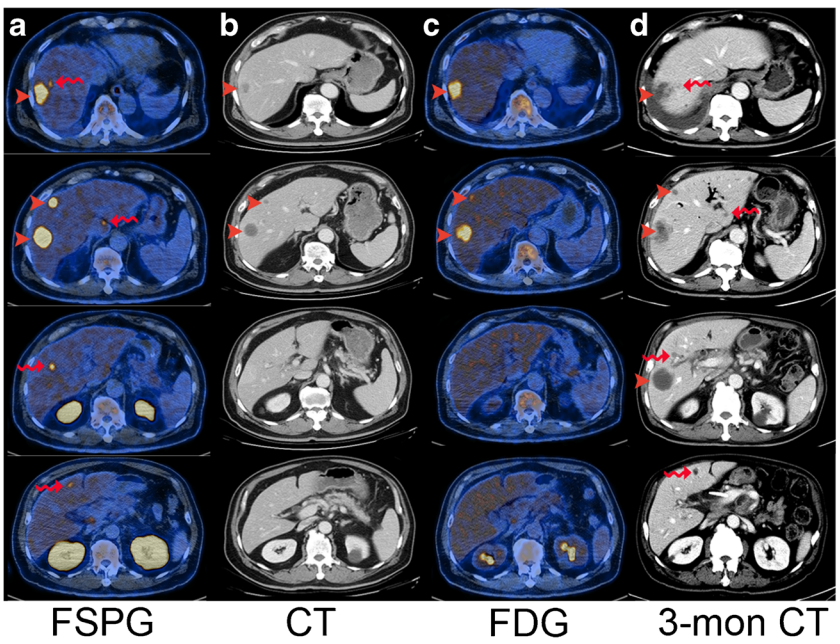

Fig. 4 ^{18}F-FSPG PET/CT (**a**), ceCT (**b**) and ^{18}F-FDG PET/CT (**c**) images, and ceCT images obtained 3 months after initial imaging (**d**), in a 75-year-old man with stage IV pancreatic cancer. ^{18}F-FSPG PET/CT consistently showed more lesions than ceCT and ^{18}F-FDG PET/CT. *Arrowheads* (▶) indicate lesions detected by ^{18}F-FSPG, ^{18}F-FDG and ceCT, and *curly arrows* (↝) indicate lesions detected only by ^{18}F-FSPG (confirmed by their appearance at corresponding locations in the liver on ceCT performed 3 months later)

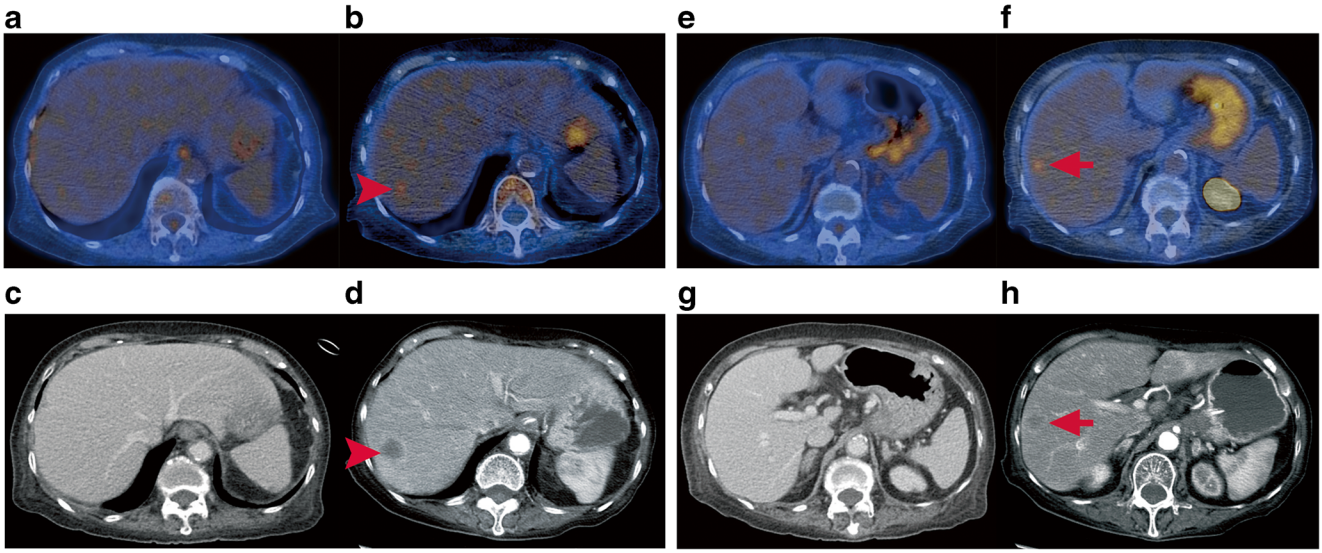

Fig. 5 Transaxial PET/CT images in an 82-year-old woman with stage III pancreatic body ductal adenocarcinoma. No hepatic metastasis are seen on the ^{18}F-FDG PET/CT images (**a**, **e**) or the contrast-enhanced abdominal CT images (**c**, **g**). The ^{18}F-FSPG PET/CT images (**b**, **f**) show at least three small foci of mild to moderate uptake in the liver (*arrows* and *arrowheads*; not all lesions are shown), suggestive of hepatic metastases. These hepatic metastases are evident on the contrast-enhanced CT images (**d**, **h**) obtained 3 months later

11 HCC patients, FSPG PET detected 75% of lesions seen on CT and MRI [17]. Therefore, our study confirmed the hypothesis that, based on tissue-specific and cancer-upregulated expression of xCT, FSPG PET performed better in detecting metastasized PDAC than in detecting breast, lung and liver cancer.

Our clinical study showed that in all patients with stage IV PDAC, liver metastases presented as hot spots on FSPG and FDG PET. Primary PDAC lesions were all FDG-avid, but showed variable uptake of FSPG. Possible explanations for primary PDAC presenting as cold areas on FSPG PET images include: (1) the fibrotic stroma in PDAC decreases tumour cellularity and hence uptake of the radiotracer is decreased, and (2) physiological expression of xCT in normal pancreatic tissue leads to high background activity and hence lesion-to-background visualization of tumour tissue is decreased. In contrast, the low background activity in the liver explains why all PDAC liver metastases presented as hot spots on FSPG PET images. The superior ability of FSPG PET over FDG PET to detect PDAC metastases may also be because expression of xCT is upregulated in cancer tissue to maintain cellular redox balance in severe conditions of oxidative stress from anaerobic metabolism [24].

Of note, uptake of radiopharmaceuticals in normal pancreas could be associated with either exocrine or endocrine physiological activity. Other authors have demonstrated decreased protein synthesis in rodents receiving a specific diet [25, 26]. Therefore, it is theoretically possible to decrease uptake of FSPG in normal pancreas by dietary restriction, thereby enhancing the tumour-to-nontumour ratio in the main pancreas. However, our FSPG PET protocol was the same as that used by Baek et al. [14], and no specific dietary restriction was instituted. This lack of dietary control may also explain the variable FSPG uptake in the main PDAC in our cohort. It would be interesting to observe the effect of specific diets on the uptake of FSPG in normal pancreas, i.e. using diet to decrease the normal physiological FSPG uptake to better visualize neoplastic pancreatic cells. Clearly, a more complete understanding of the cellular mechanisms affecting pancreatic cancer growth and FSPG uptake is needed.

xCT has been reported in stroma and immune cells and, theoretically, benign lesions with abundant stroma and immune cells will also show FSPG uptake. In this regard, patients with viral hepatitis or bile duct obstruction may show an increase in immune cells, hepatic stellate cells, and stroma. Such increases may lead to decreases in FSPG tumour-to-background ratios, and hence, increases in the rate of false-positive findings. In contrast, the mice studied were young and had healthy liver, resulting in higher FSPG tumour-to-background ratios in preclinical studies than in clinical trials. Of course, the detected lesions in our study could have been false-positive resulting from abundant stroma cells and immune cells. However, lesions seen on FSPG or FDG PET were diagnosed as metastases only if they satisfied one of the following conditions: histopathological confirmation of metastasis by biopsy, or new or enlarged tumour seen at corresponding locations on serial follow-up ceCT. Of 23 patients in our study, 5 (21.7%) were receiving treatment for chronic hepatitis B. Their tumour SUVmax or SUVR were not significantly different from those of patients without chronic liver diseases. There were no false-positive FSPG PET findings in our study cohort, probably owing to the small number of

patients enrolled since this was a proof-of-concept study; instead, one patient was found to have a hepatic abscess showing intense FDG uptake, but a cold area on FSPG PET images (Supplementary Fig. S4). Prospective studies enrolling a larger number of patients are warranted to assess the detection rate of FSPG PET in relation to chronic liver diseases.

Patients with the earliest stage of PDAC have a survival rate of only 30% [27]. This suggests that, even very early in the course of the disease, tumour cells have spread to distant parts of the body [27]. Our study suggests that FSPG PET may allow unnecessary pancreatectomy to be avoided in patients with metastases not detected on ceCT. In addition, FSPG PET indirectly examines the in vivo expression of ROS in tumours, which can potentially be used to monitor chemotherapy responses in patients with PDAC. Using FSPG PET to select and monitor patients for target therapies may also hold promise [28–30].

There were several limitations to this study. First, the small number of patients limited the statistical power. Nonetheless, this proof-of-concept study indicated the promising sensitivity of FSPG PET/CT, which requires further evaluation in a larger, adequately powered prospective cohort study. Second, histopathological confirmation of liver metastases detected by FSPG or FDG PET/CT was not possible or ethical in all patients, particularly in those with small lesions and lesions in locations where biopsy would have been difficult or risky. Even so, all lesions detected on PET but not ceCT were defined as metastases only after they were identified at corresponding locations on subsequent follow-up ceCT performed 3 and 6 months after initial imaging. This rather brief follow-up period may have led to underestimation. Moreover, in patients without histological confirmation of disease, the number of metastases present on follow-up ceCT was used as the gold standard, which would also have led to underestimation of sensitivity in this prospective study. We did not perform tissue correlation of FSPG uptake by IHC staining for xCT and CD44 because we found that normal pancreatic tissues already expressed high levels of xCT, an expression not lost during malignant transformation. Nonetheless, it would be prudent to perform such IHC staining in future prospective trials with larger numbers of patients and obtain histological verification of FSPG PET-positive lesions so as to verify the results of our study.

In summary, this prospective study confirmed that FSPG PET is a safe and effective method for detecting metastasized PDAC. FSPG PET is more sensitive than FDG PET for early detection of liver metastases. A study with a greater number of patients, especially patients with resectable PDAC, is warranted to determine the incremental effect of additional FSPG PET imaging.

Acknowledgments We appreciate the contributions of Ms. Yu-Ning Chang and Dr. Hannes Hagu for their technical support in radiotracer synthesis, and Ms. Pin-Tsen Shih, Ms. Kwanyu Lin and Mr. Chien-Chu Liu for clinical PET/CT scans. We thank the physicians who referred their patients for inclusion in this clinical trial and who reported their follow-up data.

Funding This study was funded by National Taiwan University Hospital (MOHW104-TD-B-111-04) and the Ministry of Science and Technology (MOST 103–2321-B-002-074, MOST 104–2321-B-002-075, and MOST 104–2314-B-002-134).

Compliance with ethical standards

Conflicts of interest None.

Ethical approval All procedures performed in studies involving human participants were in accordance with the ethical standards of the institutional and/or national research committee and with the principles of the 1964 Declaration of Helsinki and its later amendments or comparable ethical standards. All applicable international, national, and/or institutional guidelines for the care and use of animals were followed. All procedures performed in studies involving animals were in accordance with the ethical standards of the institution or practice at which the studies were conducted.

Informed consent Informed consent was obtained from all individual participants included in the study.

References

1. Hartwig W, Hackert T, Hinz U, Gluth A, Bergmann F, Strobel O, et al. Pancreatic cancer surgery in the new millennium: better prediction of outcome. Ann Surg. 2011;254:311–9.
2. Ryan DP, Hong TS, Bardeesy N. Pancreatic adenocarcinoma. N Engl J Med. 2014;371:1039–49.
3. Oettle H, Post S, Neuhaus P, Gellert K, Langrehr J, Ridwelski K, et al. Adjuvant chemotherapy with gemcitabine vs observation in patients undergoing curative-intent resection of pancreatic cancer: a randomized controlled trial. JAMA. 2007;297:267–77.
4. Sperti C, Pasquali C, Piccoli A, Pedrazzoli S. Recurrence after resection for ductal adenocarcinoma of the pancreas. World J Surg. 1997;21:195–200.
5. Siegel RL, Miller KD, Jemal A. Cancer statistics, 2016. CA Cancer J Clin. 2016;66:7–30.
6. Kamisawa T, Wood LD, Itoi T, Takaori K. Pancreatic cancer. Lancet. 2016;388:73–85.
7. Kelloff GJ, Hoffman JM, Johnson B, Scher HI, Siegel BA, Cheng EY, et al. Progress and promise of FDG-PET imaging for cancer patient management and oncologic drug development. Clin Cancer Res. 2005;11:2785–808.
8. Heinrich S, Goerres GW, Schafer M, Sagmeister M, Bauerfeind P, Pestalozzi BC, et al. Positron emission tomography/computed tomography influences on the management of resectable pancreatic cancer and its cost-effectiveness. Ann Surg. 2005;242:235–43.
9. Estrela JM, Ortega A, Obrador E. Glutathione in cancer biology and therapy. Crit Rev Clin Lab Sci. 2006;43:143–81.
10. Lyons SA, Chung WJ, Weaver AK, Ogunrinu T, Sontheimer H. Autocrine glutamate signaling promotes glioma cell invasion. Cancer Res. 2007;67:9463–71.

11. Sato H, Tamba M, Ishii T, Bannai S. Cloning and expression of a plasma membrane cystine/glutamate exchange transporter composed of two distinct proteins. J Biol Chem. 1999;274:11455–8.
12. Bassi MT, Gasol E, Manzoni M, Pineda M, Riboni M, Martin R, et al. Identification and characterisation of human xCT that co-expresses, with 4F2 heavy chain, the amino acid transport activity system xc-. Pflugers Arch. 2001;442:286–96.
13. Ishimoto T, Nagano O, Yae T, Tamada M, Motohara T, Oshima H, et al. CD44 variant regulates redox status in cancer cells by stabilizing the xCT subunit of system xc(−) and thereby promotes tumor growth. Cancer Cell. 2011;19:387–400.
14. Baek S, Choi CM, Ahn SH, Lee JW, Gong G, Ryu JS, et al. Exploratory clinical trial of (4S)-4-(3-[18F]fluoropropyl)-L-glutamate for imaging xC- transporter using positron emission tomography in patients with non-small cell lung or breast cancer. Clin Cancer Res. 2012;18:5427–37.
15. Koglin N, Mueller A, Berndt M, Schmitt-Willich H, Toschi L, Stephens AW, et al. Specific PET imaging of xC- transporter activity using a 18F-labeled glutamate derivative reveals a dominant pathway in tumor metabolism. Clin Cancer Res. 2011;17:6000–11.
16. Baek S, Mueller A, Lim YS, Lee HC, Lee YJ, Gong G, et al. (4S)-4-(3-18F-fluoropropyl)-L-glutamate for imaging of xC transporter activity in hepatocellular carcinoma using PET: preclinical and exploratory clinical studies. J Nucl Med. 2013;54:117–23.
17. Kavanaugh G, Williams J, Morris AS, Nickels ML, Walker R, Koglin N, et al. Utility of [(18)F]FSPG PET to image hepatocellular carcinoma: first clinical evaluation in a US population. Mol Imaging Biol. 2016;18:924–34.
18. Mittra ES, Koglin N, Mosci C, Kumar M, Hoehne A, Keu KV, et al. Pilot preclinical and clinical evaluation of (4S)-4-(3-[18F]fluoropropyl)-L-glutamate (18F-FSPG) for PET/CT imaging of intracranial malignancies. PLoS One. 2016;11:e0148628.
19. Mosci C, Kumar M, Smolarz K, Koglin N, Stephens AW, Schwaiger M, et al. Characterization of physiologic (18)F FSPG uptake in healthy volunteers. Radiology. 2016;279:898–905.
20. Cheng MF, Wang HP, Tien YW, Liu KL, Yen RF, Tzen KY, et al. Usefulness of PET/CT for the differentiation and characterization of periampullary lesions. Clin Nucl Med. 2013;38:703–8.
21. Huang YY, Chang YN, Cheng MF, Shiue CY, Tzen KY, Yen RF, et al. Device for prepare 18F-labelled glutamate derivatives and the automated equipment thereof. Intellectual Property Office, Ministry of Economic Affairs, R.O.C. https://twpat3.tipo.gov.tw/tipotwoc/tipotwekm?!!FR_201800369. Accessed 31 Dec 2018.
22. Smolarz K, Krause BJ, Graner FP, Wagner FM, Hultsch C, Bacher-Stier C, et al. (S)-4-(3-18F-fluoropropyl)-L-glutamic acid: an 18F-labeled tumor-specific probe for PET/CT imaging – dosimetry. J Nucl Med. 2013;54:861–6.
23. Lo M, Ling V, Wang YZ, Gout PW. The xc- cystine/glutamate antiporter: a mediator of pancreatic cancer growth with a role in drug resistance. Br J Cancer. 2008;99:464–72.
24. Conrad M, Sato H. The oxidative stress-inducible cystine/glutamate antiporter, system x ©) (−) : cystine supplier and beyond. Amino Acids. 2012;42:231–46.
25. Batistela E, Pereira MP, Siqueira JT, Paula-Gomes S, Zanon NM, Oliveira EB, et al. Decreased rate of protein synthesis, caspase-3 activity, and ubiquitin-proteasome proteolysis in soleus muscles from growing rats fed a low-protein, high-carbohydrate diet. Can J Physiol Pharmacol. 2014;92:445–54.
26. Chevalier L, Bos C, Gryson C, Luengo C, Walrand S, Tome D, et al. High-protein diets differentially modulate protein content and protein synthesis in visceral and peripheral tissues in rats. Nutrition. 2009;25:932–9.
27. Wang L, Yang H, Palmbos PL, Ney G, Detzler TA, Coleman D, et al. ATDC/TRIM29 phosphorylation by ATM/MAPKAP kinase 2 mediates radioresistance in pancreatic cancer cells. Cancer Res. 2014;74:1778–88.
28. Zou Z, Chang H, Li H, Wang S. Induction of reactive oxygen species: an emerging approach for cancer therapy. Apoptosis. 2017;22:1321–35.
29. Martinez-Useros J, Li W, Cabeza-Morales M, Garcia-Foncillas J. Oxidative stress: a new target for pancreatic cancer prognosis and treatment. J Clin Med. 2017;6:29.
30. Zhang L, Li J, Zong L, Chen X, Chen K, Jiang Z, et al. Reactive oxygen species and targeted therapy for pancreatic cancer. Oxidative Med Cell Longev. 2016;2016:1616781.